

Development of a Flexible Coupling Framework for Coastal Inundation Studies.

Saeed Moghimi^{a,b,*}, Andre Van der Westhuysen^{c,***}, Ali Abdolali^{c,***}, Edward Myers^{a,***}, Sergey Vinogradov^{a,***}, Zaizhong Ma^{c,***}, Fei Liu^{d,***}, Avichal Mehra^{c,***}, Nicole Kurkowski^{e,***}

^a*NOAA Coast Survey Development Laboratory, National Ocean Service, Silver Spring, USA.*

^b*University Corporation for Atmospheric Research, Boulder, USA.*

^c*NOAA Center for Weather and Climate Prediction, College Park, USA.*

^d*NOAA Earth System Research Laboratory, Boulder, USA.*

^e*NOAA Office of Science and Technology Integration, Silver Spring, USA.*

Abstract

To enable flexible model coupling in coastal inundation studies, a coupling framework based on ESMF/NUOPC technology under a common modeling framework called the NOAA Environmental Modeling System (**NEMS**) was developed. The framework is essentially a ‘software wrapper around atmospheric, wave and storm surge models that enables its components communicate seamlessly, and efficiently run in massively parallel environments. We implemented the coupled application including ADCIRC and unstructured WWAVEWATCHIII caps as well as NUOPC compliant caps to read Hurricane Weather Research and Forecasting

*Corresponding author (Saeed Moghimi; Email: Saeed.Moghimi@noaa.gov)

**Co-authors contribution:

1. **Saeed Moghimi:** Responsible for development of the ADCIRC, WW3-data and HWRF-data Caps and developing the coupled application. Writing the body of the manuscript and plotting figures.
2. **Andre Van der Westhuysen:** Responsible for unstructured WW3 cap development. Inclusion of the WW3 cap in the coupled application and running full coupled cases; manuscript preparation and analysis of the results.
3. **Ali Abdolali:** Responsible for WW3 cap development and running stand alone wave model, plotting wind and wave related parts of manuscripts, manuscript preparation and analysis of the results.
4. **Edward Myers:** Scientific support, discussion and project management;
5. **Sergey Vinogradov:** Scientific support and discussions.
6. **Zaizhong Ma:** Responsible for wind field modeling using HWRF.
7. **Fei Liu:** Support for ESMF/NUOPC cap development.
8. **Avichal Mehra:** Scientific support and project management.
9. **Nicole Kurkowski:** Scientific support and project management.

Model (HWRF) generated forcing fields. We validated the coupled application for a laboratory test and a full scale inundation case of the Hurricane Ike, 2008, on a high resolution mesh covering the whole US Atlantic coast. We showed that how nonlinear interaction between surface waves and total water level results in significant enhancements and progression of the inundation and wave action into land in and around the hurricane landfall region. We also presented that how the maximum wave setup and maximum surge regions may happen at the various time and locations depending on the storm track and geographical properties of the landfall area.

Keywords: wave-current interaction, tidal inlet, river plume, wind waves, three-dimensional circulation, wave breaking

1. Introduction

To establish a coastal flooding modeling system, several model components based on the target geographical region need to be coupled. To accurately simulate the total water level in a tropical hurricane land-falling inundation study, a dynamically coupled system of numerical models including storm surge, surface waves, inland river flooding and numerical weather prediction are necessary. On top of that based on the geographical location other model components may need to be employed. For instance, to setup an efficient coastal flooding prediction system for Alaska region, inclusion of a sea-ice model is essential.

In recent years, Earth System Models were proven to be invaluable tools that enabled us to better understand and more accurately predict our environment. Each system includes a coupled applications that consists of several model components to represent relevant physical processes. The model components are expected to interact with each other similar to what takes place in nature.

There are several Earth System Model software flavors that enable model components to communicate by importing and exporting data (Jacob et al., 2005; Valcke et al., 2012; Hill et al., 2004). The Earth System Modelling Framework (ESMF) has been utilized to develop several earth system coupled applica-

tions worldwide (e.g. Warner et al., 2008; Moghimi et al., 2012; Lemmen et al., 2017). To increase **ESMF** interoperability, the National Unified Operational Prediction Capability (**NUOPC**) consortium developed a layer consisting of a set of generic components (Theurich et al., 2016). **NUOPC** layer is a software wrap around **ESMF** and was developed collaboratively by several research and operational centers. The primary objectives behind **NUOPC** design are to be reusable, extensible and portable framework for ESM coupling.

The NOAA Environmental Modeling System (**NEMS**) is a coupled modeling infrastructure designed to address increasing needs for prediction of the earth environment at a range of time scales. **NEMS** includes several external model components that have a primary source code outside NOAA. Therefore, NOAA only needs to maintain and develop the coupling interfaces (so-called model caps) of the given modeling component. In turn, the **NEMS** ecosystem allows connecting various combinations of model components into a number of different coupled model applications to address specific environmental phenomena at specific time scales.

The present research goals are to develop a flexible and generic coupling between AAdvanced CIRCulation model (**ADCIRC**; Luettich Jr et al., 1992) and **WAVEWATCH III** (**WW3**; Tolman et al., 2009) via their respective **NUOPC** caps, and to provide an infrastructure to make future development and inclusion of various model components, such as river and inland flooding coupling, seamlessly possible. The current development of the **NUOPC** caps provides the possibility to perform dynamical coupling of **ADCIRC** and the unstructured version of **WW3**, as well as various atmospheric models **ATM**. The cap developed for **ADCIRC** is capable of importing atmospheric forcing and surface wave fields, and exporting water surface elevation and current velocity to the connected model components. Conversely, the cap developed for unstructured **WW3** imports atmospheric forcing, water levels and current, and exports the wave radiation stresses required to force **ADCIRC**.

The first application of this new coupled system is the so-called Named Storm Event Model (**NSEM**), a high-fidelity model for hindcasting coastal inun-

dation and total water level. It is being developed to meet the requirements of the NOAA’s Consumer Option for an Alternative System to Allocate Losses (COASTAL) Act of 2012. This modeling system includes **ADCIRC** as the hydrodynamic component, **WW3** as the wave model, the Hurricane Weather Research and Forecasting Model (**HWRF**) as the atmospheric component (Tallapragada et al., 2014), and in future the National Water Model (**NWM**) as the inland hydrological component (Gochis et al., 2013), see Fig. 1.

The structure of this paper is as follows. First, we describe the envisioned design of the **NEMS** **ADCIRC**-**WW3** coupled application and the methodology. Then a detailed description of the **ADCIRC** cap implementation and available coupling options is given. This is followed by a similar description of the **WW3** cap. Subsequently, we present the results of the coupled system. Finally we present verification of the coupled **ADCIRC**-**WW3** application for the laboratory flume case of Boer (1996), as well as a full scale storm surge inundation event during Hurricane Ike, 2008 in the US Gulf of Mexico.

2. Structure of the coupled application

A typical **NUOPC** application includes a number of generic components that provide an interface to the underlying **ESMF** infrastructure for generating and operating a coupled application in a fairly straightforward and seamless manner. The generic components are defined as follows:

- A *Driver* manages all the components to initialize, run, finalize and keep track of time for exchanging information among model components.
- *Connectors* are used to execute field matching, grid remapping and data redistribution among model components.
- A *Model* (cap) wraps each model component code (e.g. **ADCIRC** and **WW3**) to provide a generic interface and standard metadata suitable to be plugged into the *Driver*, and form a multi-model coupled application.

- An optional *Mediator* wraps custom coupling code to calculate quantities which includes data from several model components or requires operations such as time averaging.

The system includes methods and utilities for time management, error handling, high performance inputs/outputs (I/O), grid remapping and field interpolation. Since NUOPC is a layer around ESMF library, function calls to both NUOPC and ESMF are possible and sometimes are necessary.

In this research, we developed a NUOPC application that includes a driver, three NUOPC enabled model components and four connectors. The components are not allowed to directly access each other's data. The only way the data moves in or out of a component is via instances of an `ESMF_state` class. The state is a container that wraps native data and also includes a metadata to let the other components know about name, coordinates and decomposition of the actual packed data.

The driver component accesses `ADCIRC`, `WW3` and `ATMesh` model components via their `SetServices()` methods. It reads basic information for how to initialize and run the model components from a configuration text file (Fig. 2). The configuration file contains information about name of the model components, number of processes to be associated to each model component, the coupling time intervals, and the order of data exchange among the components. The driver also initializes the number of connectors by providing the name of the sending and receiving model components. Therefore, for a dynamical two-way coupling between two model components, two connectors are required.

The connector component initializes at the run time by matching the list of available import and export fields advertised by the model components. The connector establishes the connection based on matched import and export fields. The connector also has access to the domain decomposition and computational domain discretization of the connected model components. It will generate a remapping and necessary weight matrices for interpolation of the fields among model components at the initialization phase. In other words, the connector

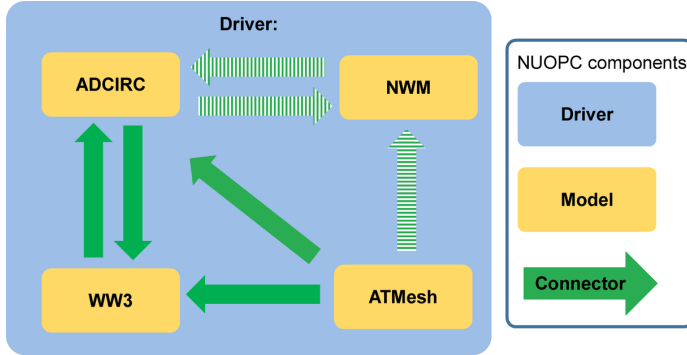


Figure 1: Design of the coupled application for coastal flooding inundation studies (NSEM).

All model configurations and results are pre-decisional and for official use only.

receives exported data in the form of an `ESMF_state` in the native grid or mesh from the exported model component and passes it to the importing model components in its own native grid or mesh definition. This remapping facility allows the coupled system the freedom to use different meshes for, say, the circulation and wave modeling components, and/or different domain decompositions. This is useful in cases where the wave model component requires a different mesh optimization to resolve its distinct physics, or more computational cores for load balancing.

The `ATMesh` cap was developed as a placeholder interface for a full live atmospheric model, which was not included in our NSEM application due to scope limitations. This so-called data cap reads weather prediction outputs (from a NetCDF data file), initialize required NUOPC/ESMF objects and provide requested data and information to `ADCIRC` and `WW3` caps via the NUOPC/ESMF backbone. The `NWM` hydrological model component and its associated connectors are not yet implemented (Fig. 1).

3. ADCIRC model

The Advanced CIRCulation model (`ADCIRC`) is a finite element hydrodynamic community model originally developed by Luettich Jr et al. (1992). `ADCIRC` is undergoing continuous development by groups of scientists and engineers. Its

natural finite element unstructured mesh capability, and several modules specifically addressing various aspects of the coastal flooding and tropical cyclone forcing, make it one of the best tools available for coastal inundation studies. **ADCIRC** operates in either two-dimensional depth-integrated (2D) depth-averaged (barotropic) and three-dimensional (baroclinic) modes. In the 2D mode, it solves equations for both water surface elevation and the depth-averaged velocity fields. For more details about **ADCIRC** governing equations, numerical methods and wave forcing implementation please see (Luettich Jr et al., 1992; Dietrich et al., 2011).

ADCIRC is written in modular **FORTRAN** and supports parallel execution on massive supercomputers using **MPI** architecture. The code structure is partitioned in three distinct initializing, running and finalizing phases ready for the **ESMF** coupling. The model initializes by a call to **ADCIRC_Init()** which also receives a **MPI** communicator from the driver. The subroutine reads necessary input files for constructing the computational mesh including nodes location and connectivity. It also builds a local and global nodal map to reference which nodes reside on which **MPI** process, and to identify their global relationships. It reads input information to constrain the model such as bathymetry, meteorological forcing, and freshwater inflow and open boundary conditions. As a part of the initialization, **ADCIRC** also checks and connects to all requested output files that will be used as containers to fill in the model results.

ADCIRC enters the run phase by a call to **ADCIRC_Run()** subroutine, which also receives an argument for the number of time steps (**NTIME_STP**) for that specific run request. The start time and end time of the simulation is determined during the initialization phase. The model run takes place via a time loop in which, at every time step, a single call to the **TIMESTEP()** subroutine occurs. All the computational steps for applying forcing and boundary conditions to produce the final results are being performed in this subroutine. The **ADCIRC** concludes its run by a call to **ADCIRC_Final()** subroutine where some of the final post-processing and check for **MPI** finalizing are performed.

```

#####
#### NEMS Run-Time Configuration File #####
#####

# EARTH #
EARTH_component_list: ATM OCN WAV
EARTH_attributes:::
  Verbosity = max
:::

# ATM #
ATM_model: atmesh
ATM_petlist_bounds: 382 382
ATM_attributes:::
  Verbosity = max
:::

# OCN #
OCN_model: adcirc
OCN_petlist_bounds: 0 381
OCN_attributes:::
  Verbosity = max
:::

# WAV #
WAV_model: ww3data
WAV_petlist_bounds: 383 383
WAV_attributes:::
  Verbosity = max
:::

# Run Sequence #
runSeq:::
@3600
  ATM -> OCN  :remapMethod=redist
  WAV -> OCN  :remapMethod=redist
  ATM
  WAV
  OCN
@:
:::

```

Figure 2: Coupled application configuration file.

All model configurations and results are pre-decisional and for official use only.

3.1. ADCIRC coupling interface (cap)

The ADCIRC NUOPC cap performs the coupling in all the three phases: initialize, run and finalize. In the development of the NUOPC cap for ADCIRC, extreme care and attention were paid to minimize changes to the original ADCIRC code. At the initialization of the NUOPC application, a global MPI communicator is created by ESMF infrastructure and a dedicated set of processes passed to ADCIRC via a MPI communicator based on the number of processes requested for ADCIRC in the configuration file. At the initialization, ADCIRC cap also gets connected to available import and export field matches accepted by the communicators.

After information exchange among the model components, the `ModelAdvance()` subroutine of the ADCIRC cap calls the `ADCIRC_Run()` subroutine to perform the next run interval. Tab. 1 shows the list of the exported and imported fields currently accepted by the ADCIRC cap. The naming conventions of these variables are defined in the NUOPC field dictionary to allow interoperability with other NUOPC components. We modified and tested ADCIRC preprocessing and main model code to accommodate various coupling arrangements. The NWS input parameters in `fort.15` input file are described in Tab. 2 (Moghimi et al., 2019).

4. WAVEWATCH III

WAVEWATCH III (WW3) (Tolman et al., 2009) is a third-generation spectral wave model that solves the wave action balance equation that accounts for the growth, propagation, non-linear interaction and dissipation of wind waves in the ocean by:

$$\frac{\partial N}{\partial t} + \nabla_x \cdot (\mathbf{c}_g + \mathbf{U})N + \frac{\partial}{\partial k} \dot{k}N + \frac{\partial}{\partial \theta} \dot{\theta}N = \frac{S}{\sigma} \quad (1)$$

where $N(k, \theta)$ is the wave action density spectrum, related to the wave energy density spectrum $F(k, \theta)$ where $N(k, \theta) = F(k, \theta)/\sigma$. Here k is the wavenumber and \dot{k} its propagation speed due to depth- or current-induced Doppler shifting, θ is the wave direction and $\dot{\theta}$ its propagation speed due to depth- or

Table 1: Exported and imported fields in coupled system.

All model configurations and results are pre-decisional and for official use only.

Data field	Units	Variable	Exported by	Imported by
Eastward sea water velocity	ms^{-1}	UU2	ADCIRC	WW3
Northward sea water velocity	ms^{-1}	VV2	ADCIRC	WW3
Sea surface height above mean sea level	m	ETA2	ADCIRC	WW3
Eastward radiation stress	$m^2s^{-2}(Nm^{-2}/\rho)$	ADCIRC_SXX	WW3	ADCIRC
Northward radiation stress	$m^2s^{-2}(Nm^{-2}/\rho)$	ADCIRC_SYY	WW3	ADCIRC
Cross radiation stress	$m^2s^{-2}(Nm^{-2}/\rho)$	ADCIRC_SXY	WW3	ADCIRC
Air pressure at sea level	mH_2O	PRN2	ATMesh	ADCIRC
Eastward wind at 10m height	ms^{-1}	WVNX2	ATMesh	ADCIRC, WW3
Northward wind at 10m height	ms^{-1}	WVNY2	ATMesh	ADCIRC, WW3

Table 2: New implemented and tested **ADCIRC** options.

All model configurations and results are pre-decisional and for official use only.

NWS parameter	Meteorological forcing	Wave forcing
17	ATM*	None
517	ATM*	WAV**
500	None	WAV**
519	Best Track (Holland Model)	WAV**
520	Best Track (Generalized Asymmetric Holland Model)	WAV**

* Any NUOPC enabled numerical weather prediction model providing required data fields e.g. **ATMesh** cap.

** Any NUOPC enabled wave model model providing required data fields e.g. **WW3** cap.

current refraction, σ is the wave frequency, \mathbf{c}_g is the group velocity, and \mathbf{U} the depth-averaged current velocity. On the right-hand side, S represents the sum of source terms, including wave growth, nonlinear interaction and dissipation. **WW3** was originally developed on a regular grid for global operational wave forecasting, with 2-way nesting for regional applications. More recently, it has been extended to curvilinear grids for Arctic applications (Rogers et al., 2018), as well as unstructured meshes for high-resolution coastal application (Ardhuin and Roland, 2013). Most recently, its traditional ‘card deck’ MPI parallel implementation (Tolman, 2002) has been supplemented with a more conventional domain-decomposition approach using ParaMETIS Roland et al. (2012) equipped with an optional implicit equation solver. Along with these improvements in numeric, source terms suitable for nearshore application have been added, including depth-induced breaking, reflection, three-wave non-linear interaction, and wave-ice interaction, amongst others.

The **WW3** code is written in modular **FORTRAN**, similar to **ADCIRC**, and is broken up into a collection of sub-programs which are run in sequence to carry out a simulation. The most important of these are **ww3_grid**, which compiles the computational mesh, and physics and numerics settings into **mod_def.ww3**, a binary resource file, **ww3_prep**, which preprocesses all forcing files, **ww3_multi**, the multi-grid core wave model, and **ww3_ounf** and **ww3_ounp**, which are NetCDF postprocessing routines. To comply with the ESMF protocol, the core wave model **ww3_multi** has been broken up into **w3init**, **w3wave**, and **w3final** to perform the main steps of model initialization, model advancing, and model finalization, respectively (Campbell and Whitcomb, 2013). During the initialization step with **w3init**, the configuration of the computational mesh file, including node indices, geographical location, and the mesh connectivity is read from the binary resource file **mod_def.ww3**. Using the domain decomposition from the **PDLIB** library, a local and global nodal map is built that references which nodes reside on which MPI process, and how they are related globally. During the model advance step **w3wave**, forcing fields such as water depth, wind velocity and currents as well as boundary conditions are updated, followed by the solution of

the wave action equation equation by means of fractional stepping. Output is written to a set of binary output files for later postprocessing (using `ww3_ounf` and `ww3_ounp`). Model finalization is completed by calling `w3final`.

4.1. *WAVEWATCH III NUOPC cap*

The `WW3` NUOPC cap carries out the coupling in the three phases (initialization, advancing and finalizing) described above. A regular grid version of this cap was developed by Campbell and Whitcomb (2013) for global and regional-scale NUOPC applications. In the present work, this cap was extended to support unstructured meshes and domain decomposition for high-resolution coastal modeling. During the initialization of the NUOPC application, import and export meshes are defined based on the PDLIB decomposition, a global MPI communicator is created by the ESMF infrastructure, and a dedicated set of processes are passes to `WW3` via a MPI communicator based on the number of processes requested for `WW3` in the configuration file (Fig. 2). During this initialization step, the `WW3` cap is also connected to available import and export field matches accepted by the communicators.

After the information exchange among the model components, the `ModelAdvance()` subroutine of the `WW3` cap calls the `w3wave` subroutine to perform the next run interval. Tab. 1 shows the list of the exported and imported fields accepted by the `WW3` cap for the current application. It is noted that a larger set of import and export variables is supported by the `WW3` cap in general, including surface roughness variables, Stokes drift and bed roughness, used in other NUOPC applications featuring wind waves. For more details, see Campbell and Whitcomb (2013).

4.2. *Wave-induced stresses*

Breaking waves transfer their momentum to ocean currents. Mathematically, this forcing is expressed in the circulation model as the divergence in the radiation stresses, as described in some detail below. From spectral wave models such as `WW3`, the radiation stress vectors can be evaluated from the computed

wave energy density as follows (Tolman et al., 2009):

$$\begin{aligned}
S_{XX} &= \rho_w g \int \int (n - 0.5 + n \cos^2(\theta)) F(k, \theta) d\theta dt \\
S_{XY} &= \rho_w g \int \int n \sin(\theta) \cos(\theta) F(k, \theta) d\theta dt \\
S_{YY} &= \rho_w g \int \int (n - 0.5 + n \sin^2 \theta) F(k, \theta) d\theta dt
\end{aligned} \tag{2}$$

where ρ_w is the water density, g is the gravitational acceleration, the directional wave energy density spectrum $F(k, \theta) = \sigma N(k, \theta)$, d is the water depth, and n is the ratio of the wave group c_g to wave phase speed c_p for a given depth and frequency, given by: $n = \frac{1}{2} + \frac{kd}{\sinh(2kd)}$.

In order to account for the impact of the waves on the mean circulation, the spatial gradient of wave radiation stress per unit area $\tau_{s,waves}$ are calculated as:

$$\begin{aligned}
\tau_{sx,waves} &= - \left(\frac{\partial S_{XX}}{\partial x} + \frac{\partial S_{XY}}{\partial y} \right) \\
\tau_{sy,waves} &= - \left(\frac{\partial S_{YY}}{\partial y} + \frac{\partial S_{XY}}{\partial x} \right)
\end{aligned} \tag{3}$$

and incorporated as additional surface stresses alongside wind stresses and bottom stresses into ADCIRC's Generalized Wave Continuity Equation and vertically-integrated momentum equations, following Dietrich et al. (2011).

5. Model setup

We utilized the existing Hurricane Surge On-demand Forecast System unstructured triangular mesh as the base of the computational domain for the coupled model setup. The HSOFS mesh covers the entire Gulf of Mexico and extends into the Atlantic Ocean to the approximate longitude of 65°W, allowing for appropriate generation of storm surge from atmospheric effects over a large region. The HSOFS mesh has 1.8 M nodes and covers the shallow coastal regions up to a topographic height of 10 m above local mean sea level with the mesh resolution of approximately 250 m (See Sec. 7.2.

6. Results

The importance of dynamical coupling of surge and surface waves on the spatial extent of the inundation and active wave action area were investigated for Hurricane Ike, 2008.

Hurricane Ike was a powerful tropical cyclone that swept through portions of the Greater Antilles and Northern America in September 2008, wreaking havoc on infrastructure and agriculture, particularly in Cuba and Texas. The ninth tropical storm, fifth hurricane, and third major hurricane of the 2008 Atlantic hurricane season, Ike developed from a tropical wave west of Cape Verde on September 1 and strengthened to a peak intensity as a Category 4 hurricane over the open waters of the central Atlantic on September 4 as it tracked westward. Several fluctuations in strength occurred before Ike made landfall on eastern Cuba on September 8. The hurricane weakened prior to continuing into the Gulf of Mexico, but increased its intensity by the time of its final landfall on Galveston, Texas on September 13.

The wave-surge coupled application (hereafter Fully coupled) and stand alone models (hereafter “Stand alone”) were forced with an identical HWRF meteorological forcing (See Sec. 7.2.1). As a reference, the ADCIRC model results forced with tidal boundary condition is also presented (hereafter “Only tide”).

The map of the maximum surge level during the whole simulation for the Fully coupled case is shown in Fig. 3a. The maximum surge level is calculated by subtracting tidal water level from Fully coupled results. The results reveal that the most severe inundation during Ike, 2008 with more than 6 m above the maximum tide level was took place on the east side of the hurricane track in the region between the Galveston Bay, Tx and the Sabine Lake, Tx.

The maximum wave contribution to total water level is calculated by subtracting Stand alone water level from Fully coupled results (Fig. 3b). It is shown that some of the wave induced inundation (wave setup) occurs at the edge of the maximum surge where the atmospheric wind setup and negative pressure

are at their maximum strength. This is significant because it shows how wave induced momentum released from breaking waves increases the total water level which in turn causes the wave active breaking region to advance further into the land and release wave action on the structures further landwards.

Wave height significantly enhanced due to the dynamical coupling of the surge and wave components. Fig. 4a, b represents the maximum wave height difference during the whole storm between Fully coupled and Stand alone (which includes no tidal or surge/inundation effects) cases. Wave height increases more than 2 m along the track as well as in the east of the Galveston Bay at the coastal and landfall region. The comparison at the 6 quick deployed wave gauges shows significant contribution of the surge on the eastern side of hurricane track in nearshore region (Fig. 17).

It should be noted that wave setup contribution seen in Fig. 3b at the Mississippi and Atchafalaya rivers delta region occurred hours before the actual landfall therefore the maximum surge and wave setup in this region did not happen at the same time. However, it also points to the possibility of experiencing large swells and rip-current events hours before hurricane makes its actual landfall.

To further analyze this mechanism, we plot changes of the total water level (TWL) and wave height for the Fully coupled and Stand alone cases at a transect shown in Fig. 6 (The location of the transect is shown in Fig. 5). We also show the topobathy values along the transect in a positive upward vertical coordinate system where $Z=0$ m located at the local mean sea level (black line in 6b). We plotted High Water Mark observations in the 1 km radius from the transect with red squares. The TWL and wave height line plots start from the land (kilometer 0) in which ground level is almost 6 m above the local mean sea level (latitude ~ 29.80 N) and continues towards the ocean to 8 m water depth (kilometer 30) in the ocean side (latitude ~ 29.55 N). Fully coupled solution for the total water level continuously show enhancement over the Stand alone results (Fig.6a). Around the shoreline where the $Z\sim 0$ m and farther off-shore, the Stand alone model show greater total water level in comparison with the

Stand alone solution. This directly relates to wave height and its dissipation shown in Fig. 6b.

We see that Stand alone model (forced without water surface elevation from surge component) shows wave height of almost zero right after waves cross the shoreline (landwards of the $Z=0$ m; Kilometer ~ 24). On the other hand, the wave height from the coupled model show significant wave height of ~ 2.2 m in the same region (landwards of the $Z=0$ m; Kilometer ~ 24). This pattern is visible for the wave height evolution even more landwards. This mechanism in which greater total water level (~ 0.5 m) leads to the potential for more active local wave generation and propagation and therefore greater wave dissipation and release wave action which re-ignite enhancement of total water level in inundated region is presented here.

We also looked at a timeseries of water level at P shown as a blue triangle in the Fig. 5. This point is located very close to the maximum spatial extent of the inundated region (Fig. 7) which is helpful to examine time variation of the total water level for Full coupled and Stand alone cases. The ground level is also plotted by a black dashed-line which shows that P is not wet before the storm as it is located ~ 3 m above the local mean sea level. During the land fall both Fully coupled and Stand alone cases produced total water level that inundated the area. Full coupled shows inundation of ~ 1 m above the ground level which is ~ 0.5 m above the water level resulted by Stand alone case at the time of the peak of the storm.

7. Model system validation

We verified the coupled **ADCIRC-WW3** application in a step-by-step manner. In the first step, we verified all the **ESMF** intermediate exchange **ESMF_state** fields before sending and after receiving by the other model component. Then we performed a basic verification using a small setup to make sure the coupled **ADCIRC-WW3** application runs smoothly. Finally, we switched to the full scale

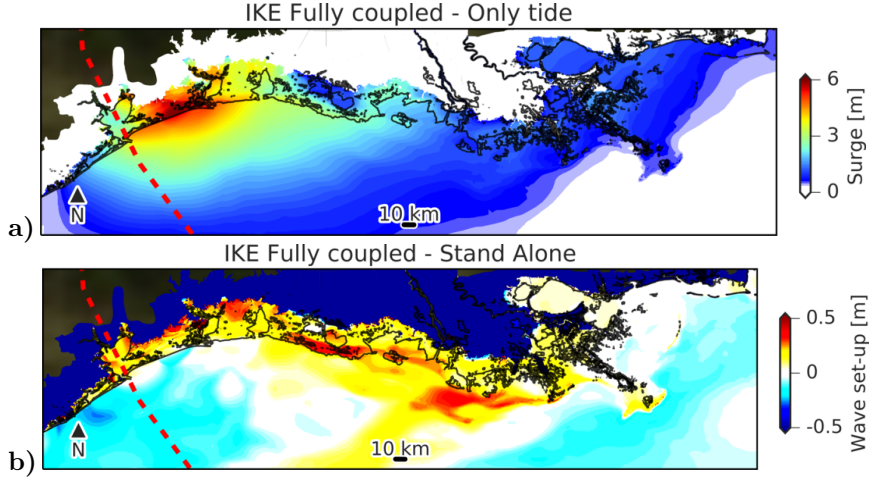


Figure 3: Total surge level computed by subtracting the tide only run from fully coupled case which includes both atmospheric and wave coupling contributions (a). The maximum wave contribution in total water level computed by subtracting stand alone case from fully coupled (b). Red line represents the Hurricane Ike best track. Black contour line represents the shoreline, and the areas beyond the black contour line are the inundated regions.

All model configurations and results are pre-decisional and for official use only.

inundation test case for Hurricane Ike, 2008.

7.1. Laboratory Case (Boers 1996)

To validate the ADCIRC-WW3 coupled system, we first compared the coupled system results against the laboratory flume experiment of Boer (1996). This experiment was carried out at Delft University of Technology in Spring 1993 to investigate the interaction between wind waves and the mean circulation via wave dissipation and radiation stress transfer. The geometry of the flume is shown in Fig. 8c. The bathymetry represents an immovable (concrete) profile of a typical barred beach along the western Dutch coastline. The Boer (1996) experiment features three test cases, 1A, 1B and 1C, in which 1A and 1B represent violently-breaking, locally-generated wind waves, and 1C represents a mildly-breaking swell. Tab. 3 shows the wave height and peak period parameters of the imposed wave conditions at the wave maker, while Fig. 9 shows their corresponding energy spectra.

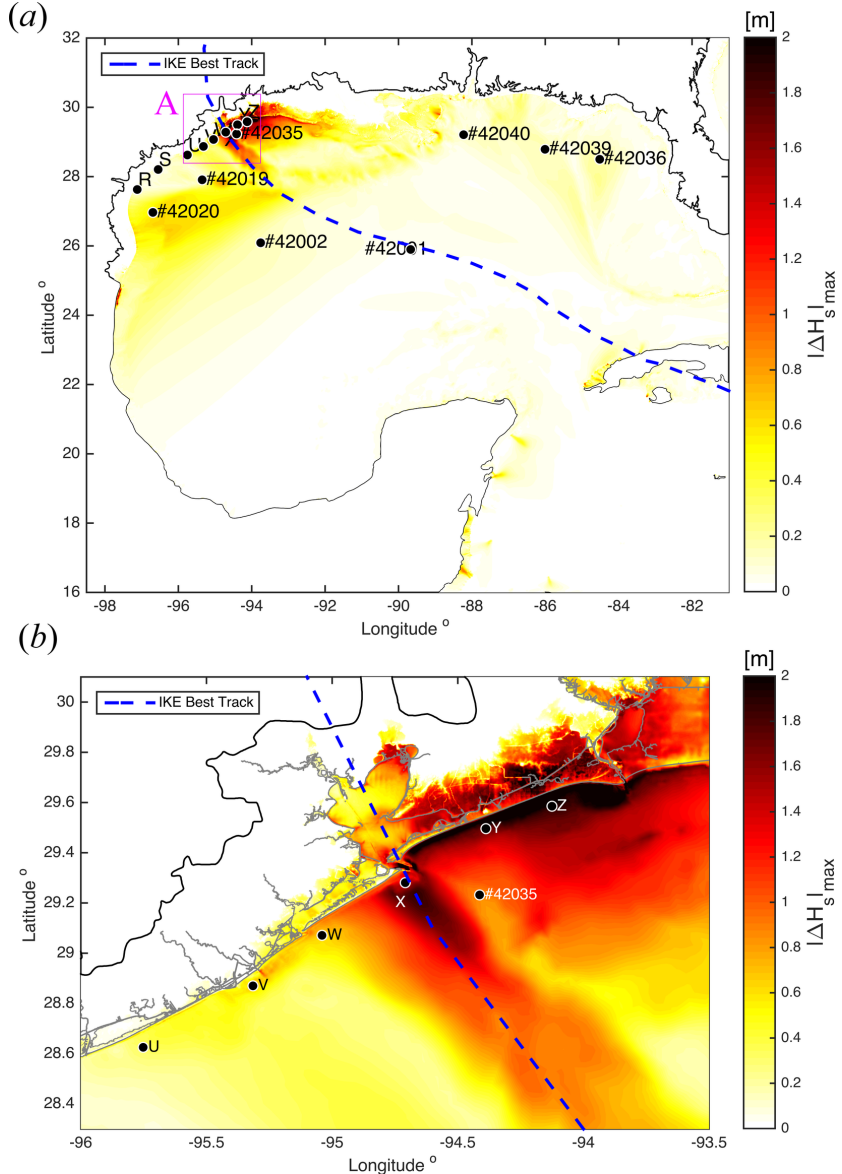


Figure 4: Wave model sensitivity to dynamic exchange between wave and surge models in term of the spatial distribution of the absolute difference between significant wave height H_s , extracted from the fully coupled Wave-Surge and Stand Alone WW3 models; Gulf of Mexico (a) landfall region (b).

All model configurations and results are pre-decisional and for official use only.



Figure 5: Red markers are the locations of the tidal gauges. The legend shows the stations ID numbers. Red dashed line is the Hurricane Ike best track. The blue line and blue triangle are transect and time serie plot shown in Fig. 6 and time series of the test point is presented in Fig. 7 respectively.

All model configurations and results are pre-decisional and for official use only.

Fig. 8a,b show the domain decompositions of the **WW3** and **ADCIRC** model components, respectively. In both cases the decomposition was generated using METIS (Karypis, 2011), but recall that in **NUOPC/ESMF** they do not necessarily need to match - for **WW3** the decomposition was done for 24 cores, while for **ADCIRC** it was done for 47 cores. The wave component of the coupled **ADCIRC-WW3** was forced with the observed spectra at the upstream wave maker, and the water level in the flume is initially set to rest. The **WW3** component is configured with a time step of 1 s. The relevant wave physics processes are depth-induced breaking and three-wave nonlinear interaction, using the source term formulations of, respectively, Battjes and Janssen (1978), with $\gamma_{BJ} = 0.80$ and $\alpha = 1$, and Eldeberky and Battjes (1996). The **ADCIRC** model component was run at a time step of 1 s, and forced from rest by only the coupled wave radiation stresses. The **NEMS** coupling time step for the two model components is 1 s.

Fig. 10 shows that the modeled significant wave heights and the wave setup produced by coupled **ADCIRC-WW3** application are in good agreement in terms of significant wave heights and the maximum water surface for all three cases. For the more energetic wave case 1B, wave heights are somewhat underestimated

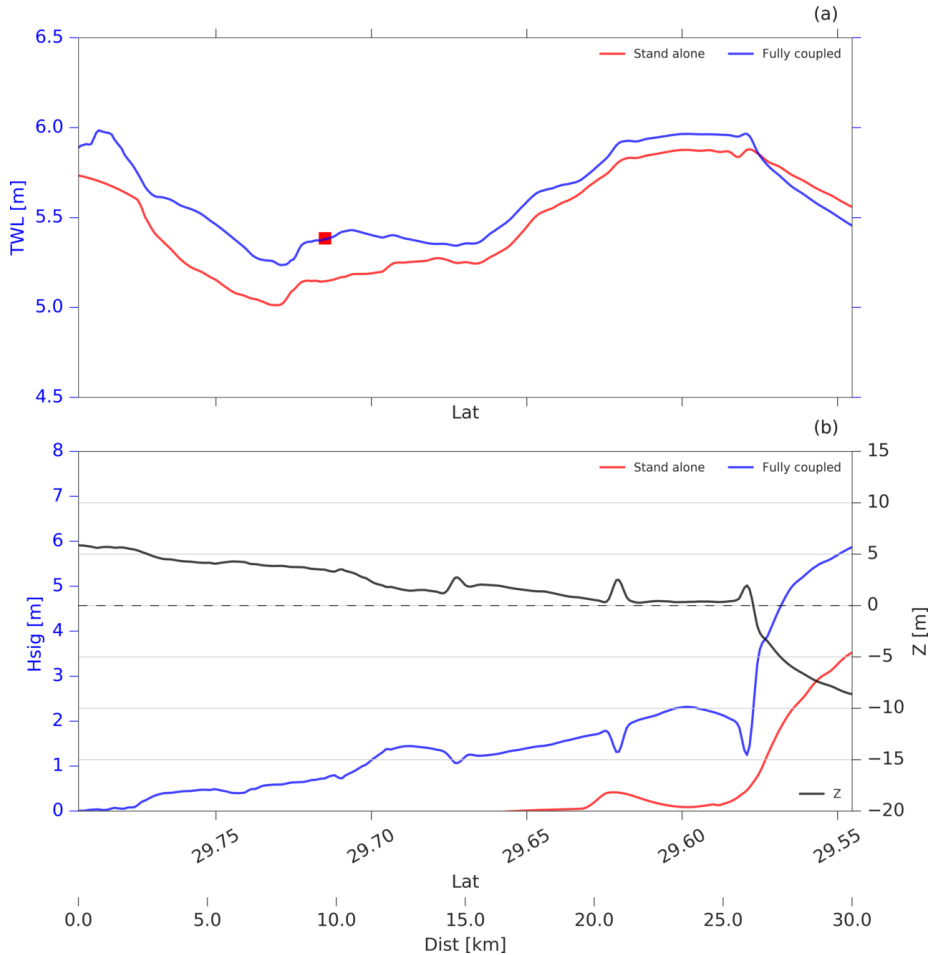


Figure 6: Comparison of the results for the transect (blue line in Fig. 5) of the total water level (a) and wave height (b) for Fully coupled and Stand alone cases are presented. The bold black line represents topobathy level referenced to the mean sea level (MSL).

All model configurations and results are pre-decisional and for official use only.

Table 3: Boers 1996 Wave conditions.

All model configurations and results are pre-decisional and for official use only.

Wave condition	H_s [m]	T_p [s]
1A	0.157	2.05
1B	0.206	2.03
1C	0.103	3.33

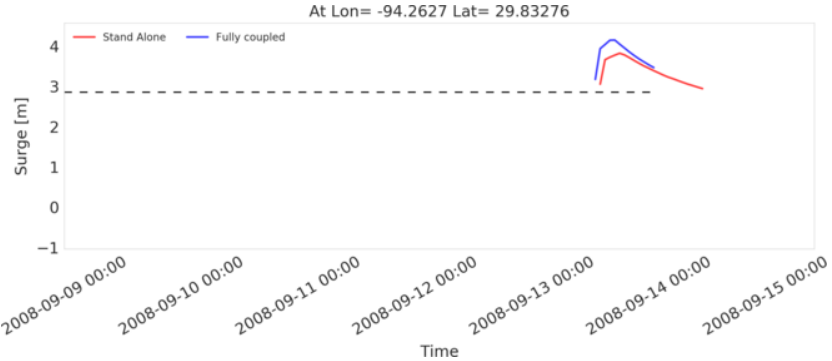


Figure 7: Time series of the total water level at the test point (locations shown in Fig. 5). Black dashed-line is the ground level.

All model configurations and results are pre-decisional and for official use only.

offshore of the outer bar. This overestimated dissipation appears to result in the overestimation of the wave setup over this region leading up to the outer bar. Conversely, in the milder-breaking swell case 1C we observe an overestimation of wave heights inshore of the outer bar, presumably due to insufficient depth-induced breaking. This results in a slight underestimation of nearshore water levels. Nevertheless, these results show good overall skill of our coupled ADCIRC-WW3 application in capturing the wave height and wave setup evolution correctly.

7.2. Full scale inundation case

Here we present the results of the full scale inundation study for Hurricane Ike, 2008. To simulate the combined waves and storm surge for Hurricane Ike, we utilized the unstructured triangular mesh used by NOAA's operational Hurricane Surge On-demand Forecast System (HSOFS). We applied 8 tidal constituents (M2, K1, O1, P1, Q1, N2, S2, K2) at the model open boundaries (Figs. 12).

7.2.1. Atmospheric forcing

The atmospheric forcing for this study is provided by NOAA's Hurricane Weather Research and Forecasting (HWRF) modeling system, coupled to the

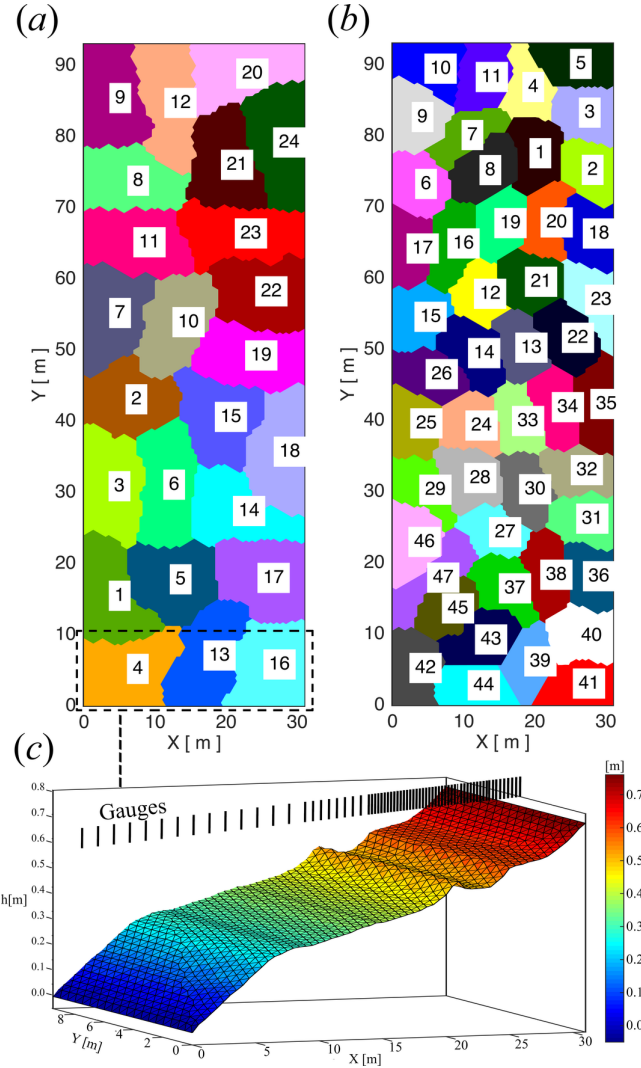


Figure 8: Schematic view of parallelization via domain decomposition algorithm in (a) WW3 with 24 subdomains; and (b) ADCIRC with 47 subdomains for Boer (1996) experiment. (c) The numerical domain with unstructured triangulated mesh.

All model configurations and results are pre-decisional and for official use only.

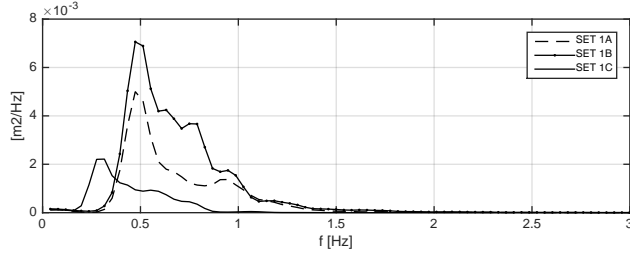


Figure 9: Energy spectra of the three different wave conditions which are summarized in Tab. 3.

All model configurations and results are pre-decisional and for official use only.

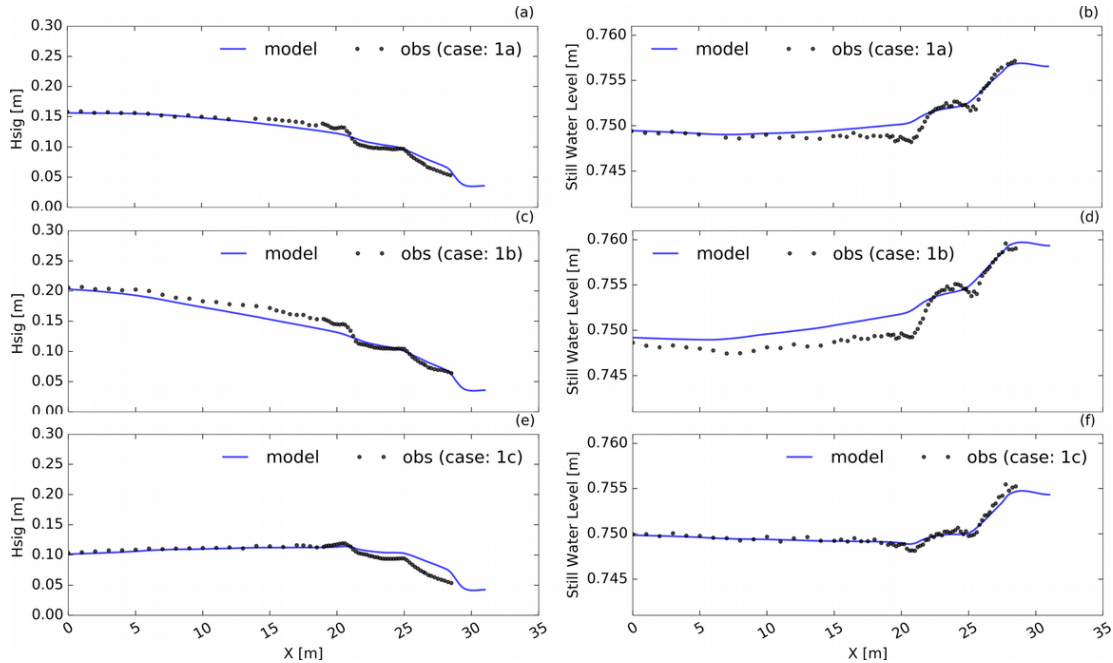


Figure 10: Significant wave height (a, c, e) and wave setup (b, d, f) for three different wave conditions which are summarized in Tab. 3.

All model configurations and results are pre-decisional and for official use only.

`MPIPOM` ocean model, and empowered by a movable multi-level nesting technology (Zhang et al., 2016; Biswas K et al., 2018). The model grid is triple-nested using telescopic, two-way interactive horizontal grid resolutions from synoptic with 0.18° resolution as the outer domain (spanning about $75^\circ \times 75^\circ$), to moving storm nest with 0.06° resolution ($10^\circ \times 10^\circ$) and core of about $6^\circ \times 6^\circ$ with 0.02° resolution. These nests follow the hurricane best track, ensuring the highest resolution around the eye of a hurricane. In this study, we have interpolated the hourly `HWRF` model outputs from multiple cycles initiated with analysis data and 9 forecast time steps. Every 6 hours, reanalysis data from the next cycle are smoothly ramped into the wind and pressure fields. The atmospheric forcing has been validated against National Data Buoy Center (NDBC) and satellite altimeter data. We extracted wind velocity at 10 m height and surface pressure from the original `GRIB2` output files and saved them in `NetCDF` format. The `ATMesh NUOPC` data cap reads the meteorological forcing from `NetCDF` file and provides it to `ADCIRC` and `WW3` caps at every coupling time step. The `HWRF` model was forced with initial and boundary conditions provided by NOAA's Global Forecast System (`GFS`) with 0.5° spatial grid resolution.

Fig. 11 gives an impression of the quality of the `HWRF` atmospheric forcing fields used to force the coupled `ADCIRC-WW3` model, by comparing 10 m wind speed and direction against NDBC buoy observations in the Gulf of Mexico (see Fig. 4 for locations). We can see that the agreement is generally good, in particular for wind directions. However, a tendency to overestimate the wind speeds at the storm peak is found at the mid-Gulf NDBC buoys 42001 and 42002, and the shelf buoy 42019. The high bias in the wind speed is particularly evident at landfall, as seen at NDBC 42035, located on the shelf just offshore of Galveston. It would be expected that these overestimated winds would lead to a degree of overestimation of the locally-generated significant wave heights. It is also worth mentioning that the NOAA buoy 42035 broke free during the storm (See Blocked`https://www.ndbc.noaa.gov/hurricanes/2008/ike/`). Therefore, the observation time series might not be at the same location of extraction coordinate from the models.

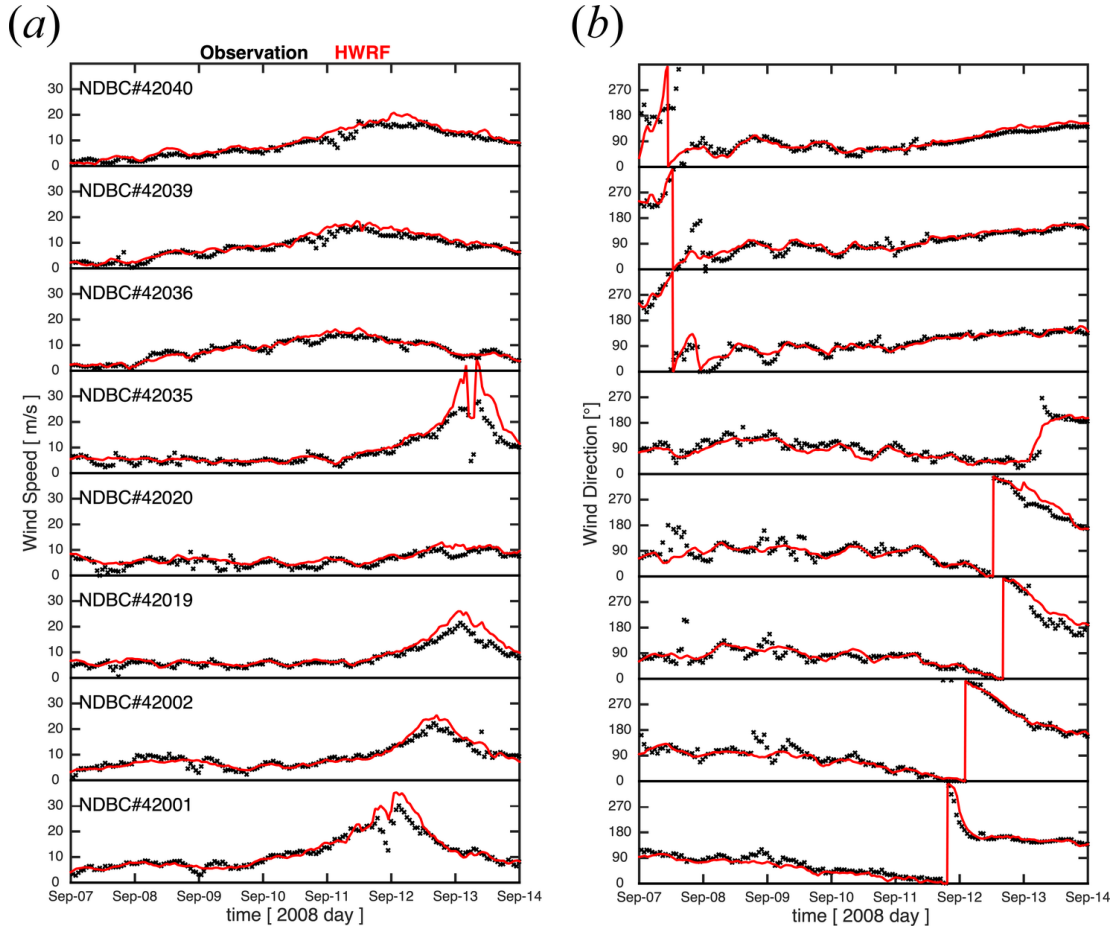


Figure 11: Atmospheric Model validation at NDBC buoy locations, Model (red) versus observation (black): (a) Wind speed (b) Wind direction.

All model configurations and results are pre-decisional and for official use only.

7.2.2. *ADCIRC* model component validation

We validated the total water level results against two sets of water level observations. The tidal gauge time-series were measured by the NOAA's Center for Operational Oceanographic Products and Services (CO-OPS) and High Water Marks (HWM) were measured and provided by United States Geographical Survey (USGS).

Comparison between the total water surface elevation from the coupled **ADCIRC-WW3** application and tidal gauges time series for four stations close to the actual hurricane track (location of the tidal gauges in Fig. 5 are presented in Fig. 13a-d). The modeled water surface elevation agrees well with the observation in terms of the level and timing of the peak of the storm inundation.

High Water Marks are an important source of observations for validation and enhancement of the storm surge and flood inundation studies. After significant flooding due to a land-falling hurricane, a rapid high water mark (HWM) data collection by USGS takes place to document the event and to help improving future disaster preparedness activities. Comparison of the total water level from the coupled **ADCIRC-WW3** application and HWMs observation reveal that both are in general agreement in particular around the hurricane track in the land-fall region (Fig. 14).

We also compared scatter plots and a number of statistical metrics of the total water levels and HWM data (Fig. 15). Both Fully coupled and Stand alone results show underestimation of the model in comparison to observations. However, upon inclusion of the wave forcing, an improvement in the error statistics is found, such that a reduction in the relative bias (RB) from -0.594 m to -0.392 m, and a reduction in root mean square error (RMSE) from 0.899 m to 0.832 m were presented.

7.2.3. *WW3* component verification

The coupled **ADCIRC-WW3** coupled application performance with respect to the wave modeling aspects was firstly assessed in the offshore and over the shelf of the Gulf of Mexico using NDBC monitoring buoys, and secondly at

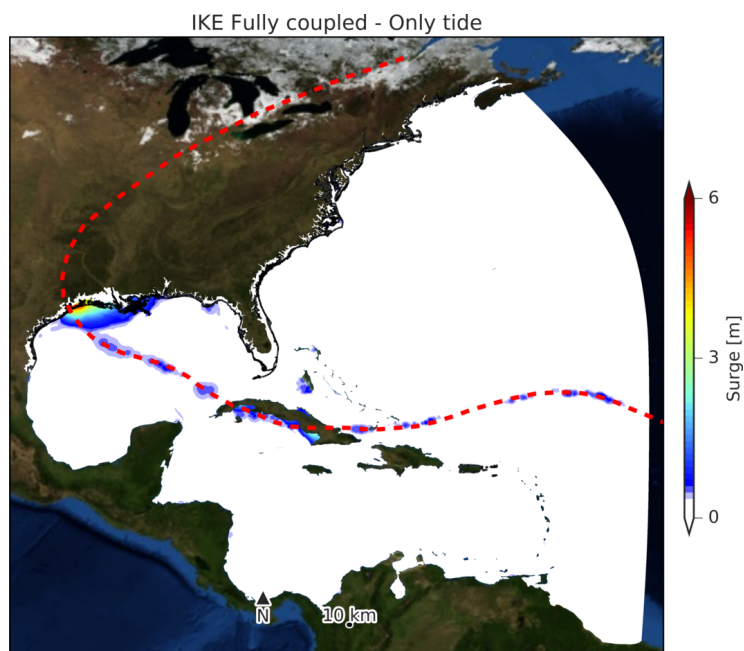


Figure 12: Surge level is computed by subtraction of tide elevation from maximum total water level for the whole HSOFS mesh. Hurricane Ikes best track is shown by a red dashed-line.
All model configurations and results are pre-decisional and for official use only.

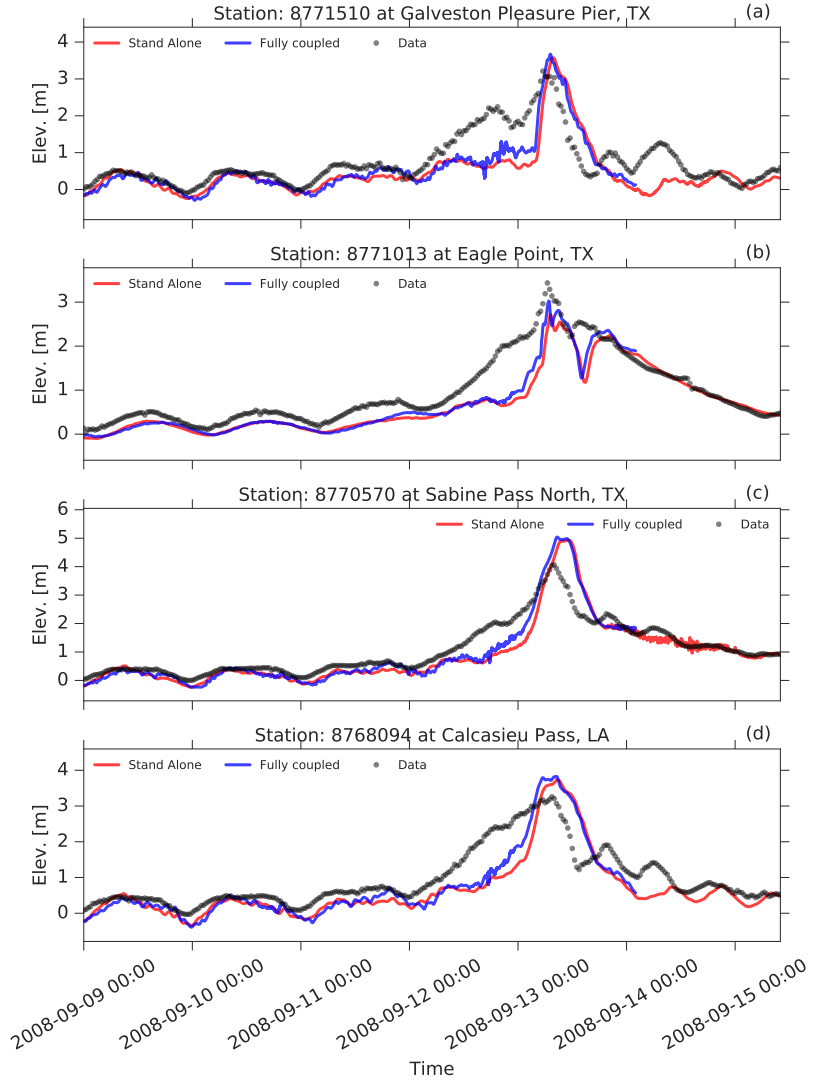


Figure 13: Time series of the total water level observations at the tidal gauges (locations shown in Fig. 5). Black dots are the observations. Red line is the tide only water level. Blue (GFS05d_OC) and green (GFS05d_OC_Wav) are storm induced total water level without and with wave forcing. Station names and ID numbers are shown in each panel titles.

All model configurations and results are pre-decisional and for official use only.

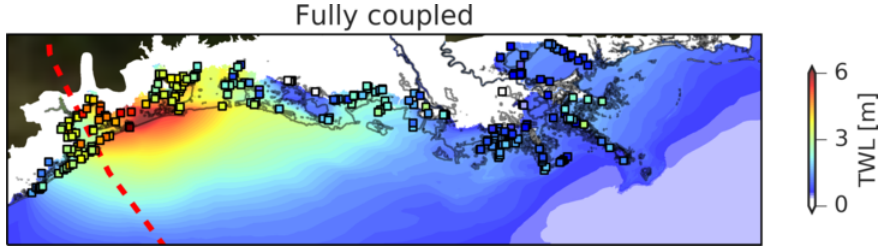


Figure 14: High water marks observations for Hurricane Ike, 2008. The contour plot is the total water level for GFS05d_OC_DA_Wav case.

All model configurations and results are pre-decisional and for official use only.

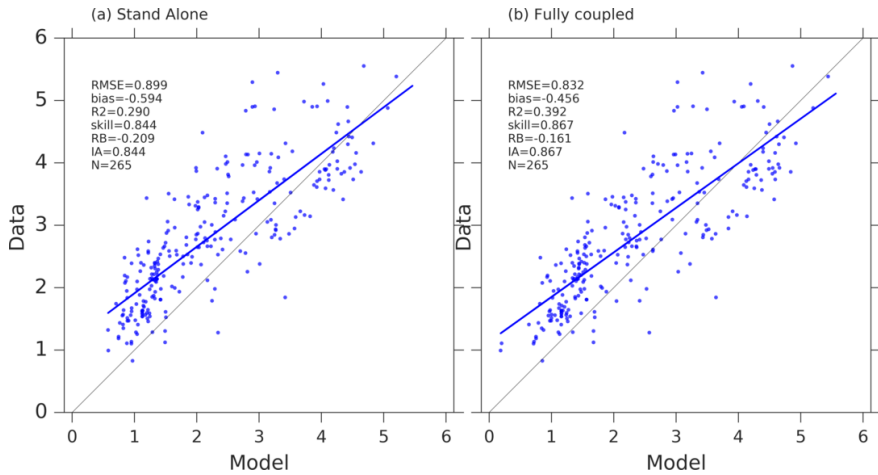


Figure 15: Statistical comparisons of High water marks observation and model results. Location of the high water mark observations are shown in Fig. 14.

All model configurations and results are pre-decisional and for official use only.

the location of landfall by using rapid-deployment pressure sensors, placed by Kennedy et al. (2011).

Considering the NDBC monitoring buoys, four groups can be distinguished. At mid-Gulf (NDBC 42001 and 42002), we find some overestimation of significant wave heights during the passing of the hurricane in response to the somewhat overestimated wind speeds seen above (Fig. 16a). Similarly, the peak wave periods are overestimated, reflecting excessive wind-sea growth (Fig. 16b). However, wave direction is reproduced well (Fig. 16c). Interestingly, in the far-field, towards the eastern half of the Gulf (NDBC 42036, 42039 42040), significant wave heights tended to be underestimated during the passing of the storm, while the peak period and direction were captured well. Moving onto the shelf in the region of landfall (NDBC 42019 and 42020) the agreement of the model results with the observations improved in general, although there is still overestimation in the significant wave height and peak period. Finally, at NDBC 42035, just offshore of the landfall location at Galveston, all wave model parameters are in good agreement with the observations at the storm peak. However, the significant wave height is underestimated at this shallow water location just ahead of the storm peak which could be related to the omission of the forerunner effect in the coupled surge model component. Regarding the differences between the coupled and stand-alone versions of the wave model, these can only be seen, as expected, at the two shallower stations NDBC 42020 and 42035. As expected, the increased water levels seen above increase the modeled significant wave height at these stations.

It should be noted that our concentration here is to ascertain general performance of the coupled model. In terms of forerunner, we reference our reader to Kennedy et al. (2011). We diagnose the forerunner surge as being generated by Ekman setup on the wide and shallow shelf. The longer forerunner time scale additionally served to increase water levels significantly in narrow-entranced coastal bays.

Moving more towards shoreline, model results at the pressure sensors deployed in the surf zone by Kennedy et al. (2011) show a significant sensitivity

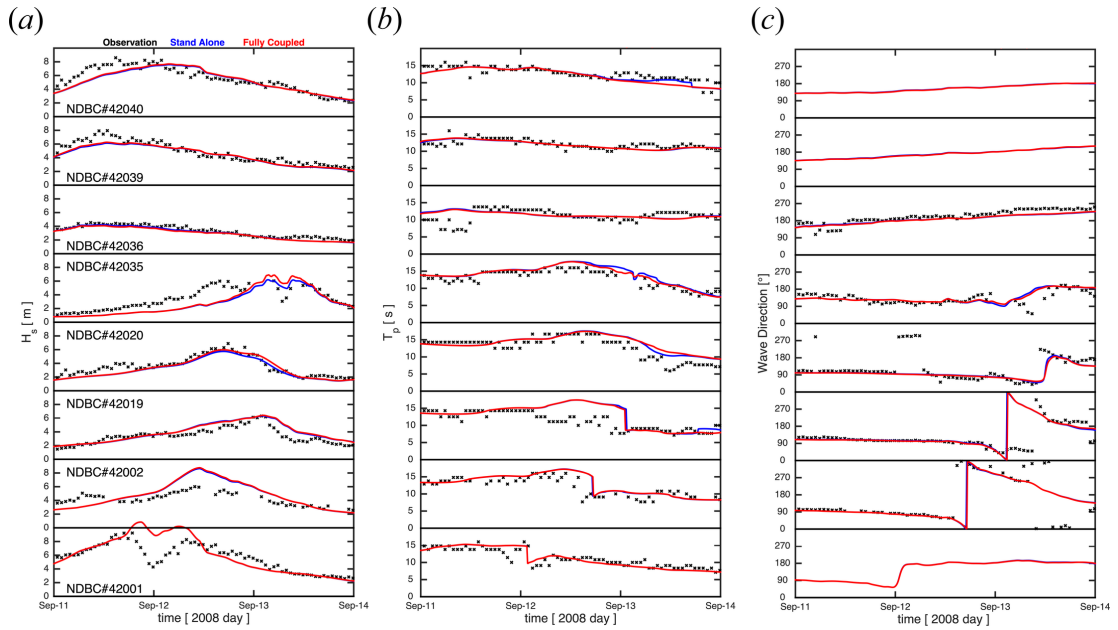


Figure 16: Model validation at NDBC buoy locations, forced by HWRF atmospheric model, extracted from stand-alone WW3 simulations (blue), fully coupled Wave-Surge simulation (red) versus observation (black): (a) Significant wave height (H_s); (b) peak period (T_p) and (c) mean wave direction. All model configurations and results are pre-decisional and for official use only.

All model configurations and results are pre-decisional and for official use only.

to the inclusion of variable water levels from the coupled ADCIRC model (Fig. 17). Referring to Fig. 4b for the station locations, the most significant of these are the stations ANDKNDY-X, Y and Z located under the eastern half of the landfalling hurricane. For these three stations, we can see a large influence of the added surge level on the significant wave height at the storm peak, in all cases improving the agreement with observations. We note that, as discussed above, the stations U to Z also might relate to underestimation of the water surface elevation during forerunner. Stations S and R, located to the south of the landfall location received mostly offshore winds and a water level set-down. The significant wave heights at these stations are reproduced well.

Fig. 18 provide a more in-depth view of the results at the Kennedy et al. (2011) nearshore stations by considering their spectrograms. This figure shows a number of important features of the nearshore wave field transformation under both the coupled and stand-alone models. Up to September 13, the simulated variance density at the northerly stations ANDKNDY-X, Y and Z is under-estimated by both the stand-alone (Fig. 18b) and coupled (Fig. 18c) models in connection with non-resolved forerunner effects. After September 13, the variance density abruptly increases, as the main storm peak arrives with landfall. At this time, the coupled model (panel c) shows greater levels of variance density than the stand-alone model (panel b), which agrees better with the observations. A final important feature of the nearshore spectra is the frequency upshift of the spectral peak, due to the nonlinear three-wave interactions. This strong upshift at stations V, W, X, Y, Z is not seen as intensely in the model results, indicating an underestimation of the magnitude of this process by the LTA nonlinear interaction source term. Interestingly, the stand-alone model captured this upshift process somewhat better than the coupled model, since the depth underestimation in the former fortuitously enhances the computed nonlinear interaction (see stations X, Y, Z).

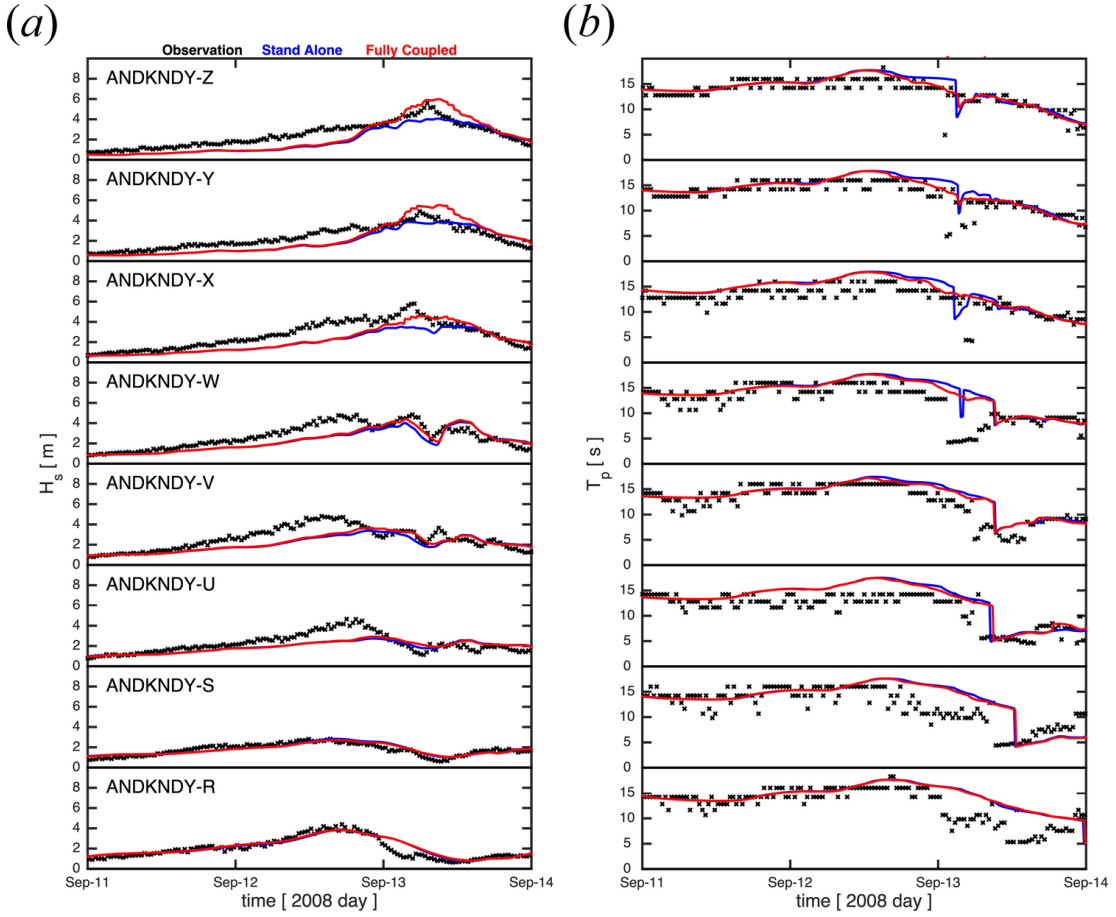


Figure 17: Model validation at quick deployed gauges, forced by HWRF atmospheric model, extracted from stand-alone WW3 simulations (blue), fully coupled Wave-Surge simulation (red) versus observation (black): (a) Significant wave height (H_s); and (b) peak period (T_p). All model configurations and results are pre-decisional and for official use only.

All model configurations and results are pre-decisional and for official use only.

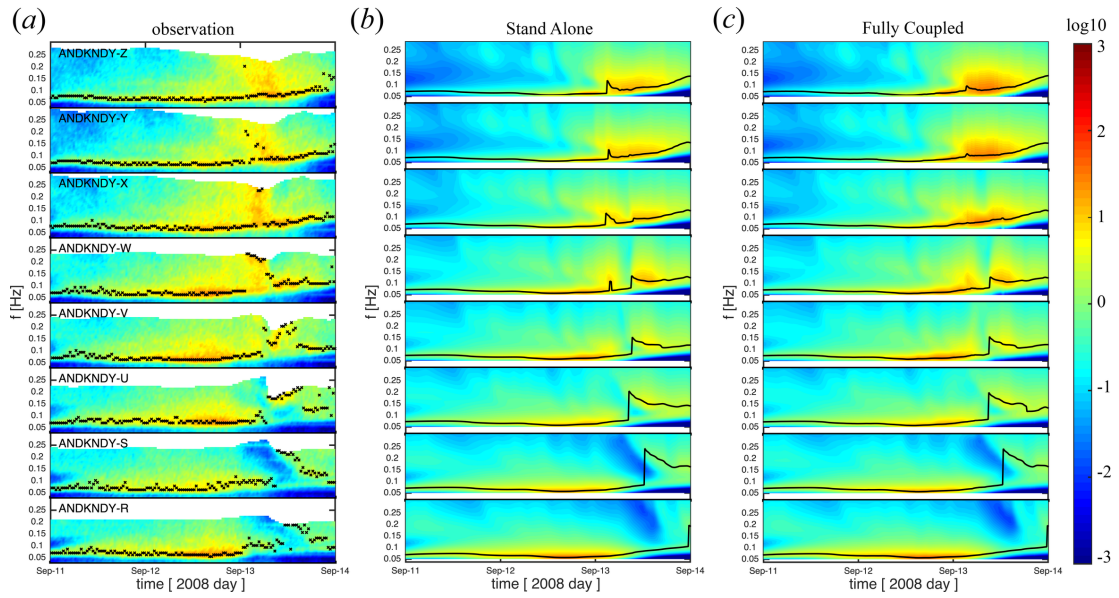


Figure 18: Frequency spectrum at nearshore quick deployed gauges comparing observation (a) versus stand-alone WW3 simulations (b) and fully coupled Wave-Surge simulation (c). The time series of peak frequency is shown in each subplot. All model configurations and results are pre-decisional and for official use only.

All model configurations and results are pre-decisional and for official use only.

8. Summary and Conclusions

We developed a flexible coupling application for coastal inundation studies in the framework of **NEMS** using **NUOPC/ESMF** infrastructure. This application includes **NUOPC** model interfaces (or caps) for **ADCIRC** and **WW3**, and also a data cap to read and provide atmospheric forcing fields from **HWRF** model results. The application is examined using a standard laboratory flume case for set-up and wave dissipation, and validated for Hurricane Ike, 2008 on NOAA's HSOFS mesh, a 1.8 M node triangular mesh with a nominal resolution of \sim 500 m. The model skills and improvement due to wave effects on the final inundation were examined and discussed using time series from tide gauges and high water marks observations.

In general, it can be concluded that the coupling improves the performance of the **ADCIRC** and **WW3** model components. The Boer (1996) case shows that the coupling between these two models behaves correctly under laboratory conditions. In the Ike field case, the simulated water levels of **ADCIRC** showed generally better agreement with observations upon inclusion of the coupled wave effects from **WW3**. Accounting for the forerunner effect is expected to improve the results further. Conversely, the coastal wave field simulated by **WW3** improves significantly upon coupling with **ADCIRC**, in particular in the surf zone and in inundated regions.

As outlined in the Introduction, the first application of the **NUOPC** model combination (or App) described here is the Named Storm Event Model (NSEM), a high-resolution hindcast model which is being developed to meet the requirements of the COASTAL Act (2012). However, we anticipate that these flexible and generic **NUOPC** coupling caps for **ADCIRC** and **WW3** will enable future development and seamless inclusion of various additional model components for forecasting applications. For example, the current cap development provides the possibility to perform three-way dynamical coupling of **ADCIRC**, **WW3** and atmospheric prediction models. In the hindcast application described here, we limited the atmospheric model, run offline, to a one-way forcing to **ADCIRC-WW3** via a

data cap. However, the **ADCIRC** and **WW3** caps are capable of dynamically importing atmospheric model forcing, and exporting current velocity, water surface elevation (accounting for inundated zones which alter the surface roughness), and enhanced sea surface roughness due to the presence of waves (Charnock parameter) back to the connected atmospheric model component.

Further future coastal applications of the presented flexible **NUOPC** modeling framework are incorporating processes such as river and inland flooding and sea ice. As part of the Named Storm Event Model, work is currently under way to incorporate river flow into this coupled system by including a **NUOPC** cap for **WRFHydro**. This extension will allow the modeling of complex coastal flooding events such as Hurricane Harvey (2017), which featured extreme rainfall and inland flooding alongside the surge and wave forcing from the ocean. Sea ice has significant and complex impacts on coastal surge (Westerink et al., 2018) as well as dissipative and dispersive effects on the coastal wave field (Rogers et al., 2018). The flexible coastal modeling system presented here can be extended to include these coupled processes via an existing **NUOPC** cap for the sea ice model **CICE** (Campbell and Whitcomb, 2013).

Acknowledgements

This work has been supported by The Consumer Option for an Alternative System to Allocate Losses (COASTAL) Act Program and Water Initiative project within the National Oceanic and Atmospheric Administration (NOAA). The WaveWatchIII development has been supported by the US. Army Corps of Engineers (USACE). The authors acknowledge Dr. Andrew Kennedy for providing the in-situ data. The results presented here are preliminary and for presenting the incremental developments of coupled application which is under development to serve above mentioned projects. The authors also would like to acknowledge Dr. Chris Massey for his constructive communications.

References

Ardhuin, F., Roland, A., 2013. The development of spectral wave models: coastal and coupled aspects, in: Proceedings of Coastal Dynamics, pp. 25–38.

Biswas K, M., Bernardet, L., Abarca, S., Ginis, I., Grell, E., Kalina, E., Kwon, Y., Liu, B., Liu, Q., Marchok, T., Mehra, A., Newman, K., Sheinin, D., Sippel, J., Subramanian, S., Tallapragada, V., Thomas, B., Tong, M., Trahan, S., Wang, W., Yablonsky, R., Zhang, X., Zhang, Z., 2018. Hurricane Weather and Research and Forecasting (HWRF) Model: 2017 scientific documentation. Technical Report. Development Testbed Center, UCAR.

Boer, M., 1996. Simulation of a surf zone with a barred beach. Report 1. Wave heights and wave breaking. Technical Report. Dept. of Civil Engineering, Delft University of Technology.

Campbell, T.J., Whitcomb, T.R., 2013. Coupling Infrastructure and Interoperability Layer Extension Across All Earth System Components. Technical Report. NAVAL RESEARCH LAB STENNIS DETACHMENT STENNIS SPACE CENTER MS.

Dietrich, J., Zijlema, M., Westerink, J., Holthuijsen, L., Dawson, C., Luettich, R.A., Jensen, R., Smith, J., Stelling, G., Stone, G., 2011. Modeling hurricane waves and storm surge using integrally-coupled, scalable computations. *Coastal Engineering* 58, 45–65.

Eldeberky, Y., Battjes, J.A., 1996. Spectral modeling of wave breaking: Application to boussinesq equations. *Journal of Geophysical Research: Oceans* 101, 1253–1264.

Gochis, D., Yu, W., Yates, D., 2013. The wrf-hydro model technical description and users guide, version 1.0. NCAR technical document 120.

Hill, C., DeLuca, C., Balaji, Suarez, M., Silva, A.d., 2004. The architecture of the earth system modeling framework. *Computing in Science & Engineering* 6, 18–28.

Jacob, R., Larson, J., Ong, E., 2005. $M \times N$ communication and parallel interpolation in Community Climate System Model version 3 using the Model Coupling Toolkit. *International Journal of High Performance Computing Applications* 19, 293–307.

Karypis, G., 2011. METIS and ParMETIS, in: *Encyclopedia of parallel computing*. Springer, pp. 1117–1124.

Kennedy, A.B., Gravois, U., Zachry, B.C., Westerink, J.J., Hope, M.E., Dietrich, J.C., Powell, M.D., Cox, A.T., Luettich, R.A., Dean, R.G., 2011. Origin of the hurricane ike forerunner surge. *Geophysical Research Letters* 38.

Lemmen, C., Hofmeister, R., Klingbeil, K., Nasermoaddeli, M.H., Kerimoglu, O., Burchard, H., Kösters, F., Wirtz, K.W., 2017. Modular system for shelves and coasts (mossco v1. 0)-a flexible and multi-component framework for coupled coastal ocean ecosystem modelling. *arXiv preprint arXiv:1706.04224* .

Luettich Jr, R.A., Westerink, J.J., Scheffner, N.W., 1992. ADCIRC: An Advanced Three-Dimensional Circulation Model for Shelves, Coasts, and Estuaries. Report 1. Theory and Methodology of ADCIRC-2DDI and ADCIRC-3DL. Technical Report. COASTAL ENGINEERING RESEARCH CENTER VICKSBURG MS.

Moghimi, S., klingbeil, K., Graewe, U., Burchard, H., 2012. Three dimensional wave current interaction in nearshore regions, in: JONSMOD2012 , Brest, France.

Moghimi, S., Vinogradov, S., Myers, E.P., Funakoshi, Y., Van der Westhuysen, A.J., Abdolali, A., Ma, Z., Liu, F., et al., 2019. Development of a Flexible Coupling Interface for ADCIRC Model for Coastal Inundation Studies. Technical Report. NOAA National Ocean Service.

Rogers, W., Posey, P., Li, L., Allard, R., 2018. Forecasting and Hindcasting Waves In and Near the Marginal Ice Zone: Wave Modeling and the ONR Sea

State Field Experiment. Technical Report. NAVAL RESEARCH LAB STENNIS DETACHMENT STENNIS SPACE CENTER MS STENNIS SPACE .

Roland, A., Zhang, Y.J., Wang, H.V., Meng, Y., Teng, Y.C., Maderich, V., Brovchenko, I., Dutour-Sikiric, M., Zanke, U., 2012. A fully coupled 3d wave-current interaction model on unstructured grids. *Journal of Geophysical Research: Oceans* 117.

Tallapragada, V., Kieu, C., Kwon, Y., Trahan, S., Liu, Q., Zhang, Z., Kwon, I.H., 2014. Evaluation of storm structure from the operational hwrf during 2012 implementation. *Monthly Weather Review* 142, 4308–4325.

Theurich, G., DeLuca, C., Campbell, T., Liu, F., Saint, K., Vertenstein, M., Chen, J., Oehmke, R., Doyle, J., Whitcomb, T., et al., 2016. The earth system prediction suite: toward a coordinated us modeling capability. *Bulletin of the American Meteorological Society* 97, 1229–1247.

Tolman, H.L., 2002. Distributed-memory concepts in the wave model WAVEWATCH III. *Parallel Computing* 28, 35 – 52.

Tolman, H.L., et al., 2009. User manual and system documentation of wave-watch iii tm version 3.14. *Technical note, MMAB Contribution* 276, 220.

Valcke, S., Balaji, V., Craig, A., DeLuca, C., Dunlap, R., Ford, R., Jacob, R., Larson, J., O'Kuinghttons, R., Riley, G., et al., 2012. Coupling technologies for earth system modelling. *Geoscientific Model Development* 5, 1589.

Warner, J., Sherwood, C., Signell, R., Harris, C., Arango, H., 2008. Development of a three-dimensional, regional, coupled wave, current, and sediment-transport model. *Computers & Geosciences* 34, 1284–1306.

Westerink, J.J., Joyce, B., Grumbine, R., van der Westhuysen, A., Feyen, J., Pringle, W.J., Wirasaet, D., 2018. Coupled tides, storm surge and waves under varying ice coverages along alaskas bering and chukchi coasts. *Coastal Engineering Proceedings* 1, 69.

Zhang, X., Gopalakrishnan, S.G., Trahan, S., Quirino, T.S., Liu, Q., Zhang, Z., Alaka, G., Tallapragada, V., 2016. Representing multiple scales in the hurricane weather research and forecasting modeling system: Design of multiple sets of movable multilevel nesting and the basin-scale hwrf forecast application. *Weather and Forecasting* 31, 2019–2034.

Appendix A: Metrics for the evaluation of data-model agreement

In order to assess model performance for water levels, root mean square error (RMSE), BIAS, relative BIAS (RB), Correlation (Cor), Index of Agreement (IA) and peak error (Peak) were used.

The RMSE is given by

$$RMSE = \sqrt{\frac{1}{N} \sum_{i=1}^N (M_i - O_i)^2} \quad (4)$$

where M_i is the modeled data, O_i is the measured data and N is the total number of data.

BIAS shows the systematic deviation from the observations and is given by

$$BIAS = \sum_{i=1}^N (M_i - O_i) \quad (5)$$

Relative BIAS (RB) shows relative systematic deviation from the observations and is given by

$$RB = \frac{\sum_{i=1}^N (M_i - O_i)}{N \langle O_i \rangle} \quad (6)$$

Peak error is calculated by

$$PEAK = \max O - \max M \quad (7)$$

The Index of Agreement (IA) is formulated as

$$IA = 1 - \frac{\sum_{i=1}^N (M_i - O_i)^2}{\sum_{i=1}^N \left((|M_i - \langle O \rangle| + |O_i - \langle O \rangle|)^2 \right)} \quad (8)$$

where brackets, $\langle \cdot \rangle$, denote time averaging. $IA = 1$ shows perfect agreement and $IA = 0$ means complete disagreement.

The Pearson correlation (Cor) coefficient is calculated by

$$Cor = \frac{\sum_{i=1}^N (O_i - \langle O \rangle)(M_i - \langle M \rangle)}{\sqrt{\sum_{i=1}^N (O_i - \langle O \rangle)^2 \sum_{i=1}^N (M_i - \langle M \rangle)^2}} \quad (9)$$

It has a value between $+1$ and -1 , where $+1$ is total positive linear correlation, 0 is no linear correlation, and -1 is total negative linear correlation